JOC Article

Coupling-Isomerization−*N*,*S*-Ketene Acetal-Addition Sequences−A Three-Component Approach to Highly Fluorescent Pyrrolo[2,3-*b*]pyridines, [1,8]Naphthyridines, and Pyrido[2,3-*b*]azepines

Oana G. Schramm, née Dediu, Thomas Oeser,† and Thomas J. J. Müller*

Organisch-Chemisches Institut der Ruprecht-Karls-Universität Heidelberg, Im Neuenheimer Feld 270, D-69120 Heidelberg, Germany

thomas_j.j.mueller@urz.uni-heidelberg.de

Received February 9, 2006

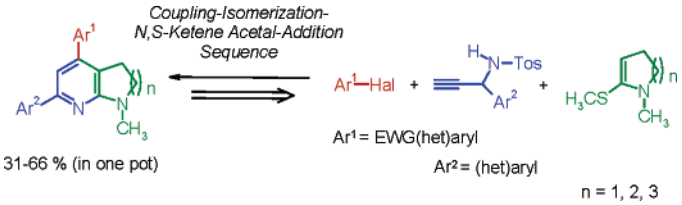

Annelated 2-amino pyridines such as pyrrolo[2,3-*b*]pyridines, [1,8]naphthyridines, and pyrido[2,3-*b*]-azepines can be synthesized in moderate to good yields in a consecutive one-pot three-component process by a coupling-isomerization−enamine-addition−cyclocondensation sequence of an electron-poor (hetero)-aryl halide, a terminal propargyl *N*-tosylamine, and an *N*,*S*-ketene acetal. After the coupling-isomerization sequence, a Diels−Alder reaction with inverse electron demand of the intermediate enimine and the *N*,*S*-ketene acetal and subsequent aromatization furnish annelated 2-amino pyridines **4** that were unambiguously characterized by numerous X-ray structure analyses. These heterocycles are highly fluorescent and partially pH sensitive, and their electronic structure was studied with spectroscopic and computational methods.

Introduction

One-pot multicomponent processes address very fundamental principles of synthetic efficiency and reaction design and, therefore, have recently gained a considerable and steadily increasing academic, economic, and ecological interest.[1,2] They are diversity-oriented syntheses[3] that can be often developed into combinatorial and solid-phase strategies,[2d,4] promising manifold opportunities for generating novel lead structures of pharmaceuticals, catalysts, and even novel molecule-based materials. As part of our program, designed to develop new multicomponent methodologies initiated by transition-metal-catalyzed C−C-bond formation, we have recently discovered and developed an unusual mode of alkyne activation by a detouring outcome of the Sonogashira coupling,[5] that is, a coupling-isomerization reaction (CIR).[6] The CIR of electron-deficient (hetero)aryl halides and (hetero)arylpropargyl alcohols or *N*-tosylamines under the conditions of the Sonogashira

† X-ray structure analyses.

(1) For a recent monography, see for example: *Multicomponent Reactions*; Zhu, J., Bienaymé, H., Eds., Wiley-VCH: Weinheim, Germany, **2005**.

(2) For reviews, see for example: (a) Bienaymé, H.; Hulme, C.; Oddon, G.; Schmitt, P. *Chem.−Eur. J.* **2000**, *6*, 3321−3329. (b) Dömling, A.; Ugi, I. *Angew. Chem., Int. Ed.* **2000**, *39*, 3168−3210. (c) Ugi, I.; Dömling, A.; Werner, B. *J. Heterocycl. Chem.* **2000**, *37*, 647−658. (d) Weber, L.; Illgen, K.; Almstetter, M. *Synlett* **1999**, 366−374. (e) Armstrong, R. W.; Combs, A. P.; Tempest, P. A.; Brown, S. D.; Keating, T. A. *Acc. Chem. Res.* **1996**, *29*, 123−131. (f) Ugi, I.; Dömling, A.; Hörl, W. *Endeavour* **1994**, *18*, 115−122. (g) Posner, G. H. *Chem. Rev.* **1986**, *86*, 831−844.

(3) For reviews on diversity-oriented syntheses, see for example: (a) Schreiber, S. L.; Burke, M. D. *Angew. Chem., Int. Ed.* **2004**, *43*, 46−58. (b) Burke, M. D.; Berger, E. M.; Schreiber, S. L. *Science* **2003**, *302*, 613−618. (c) Arya, P.; Chou, D. T. H.; Baek, M. G. *Angew. Chem., Int. Ed.* **2001**, *40*, 339−346. (d) Cox, B.; Denyer, J. C.; Binnie, A.; Donnelly, M. C.; Evans, B.; Green, D. V. S.; Lewis, J. A.; Mander, T. H.; Merritt, A. T.; Valler, M. J.; Watson, S. P. *Prog. Med. Chem.* **2000**, *37*, 83−133. (e) Schreiber, S. L. *Science* **2000**, *287*, 1964−1969.

(4) Kobayashi, S. *Chem. Soc. Rev.* **1999**, *28*, 1−15.

(5) For lead reviews on Sonogashira couplings, see for example: (a) Takahashi, S.; Kuroyama, Y.; Sonogashira, K.; Hagihara, N. *Synthesis* **1980**, 627−630. (b) Sonogashira, K. In *Metal Catalyzed Cross-coupling Reactions*, Diederich, F., Stang, P. J., Eds.; Wiley-VCH: Weinheim, Germany, **1998**, 203−229. (c) Sonogashira, K. *J. Organomet. Chem.* **2002**, *653* (1−2), 46−49. (d) Negishi, E.-I.; Anastasia, L. *Chem. Rev.* **2003**, *103*, 1979−2018.

(6) Müller, T. J. J.; Ansorge, M.; Aktah, D. *Angew. Chem., Int. Ed.* **2000**, *39*, 1253−1256.

10.1021/jo0602726 CCC: $33.50
Published on Web 03/29/2006

SCHEME 1. Coupling-Isomerization Reaction (CIR), a Novel Synthesis of Enones and Enimines[a]

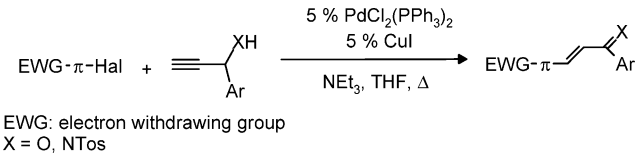

[a] EWG: electron-withdrawing group; X = O, NTos.

coupling is a mild and efficient route to chalcones[6] or enimines,[7] respectively (Scheme 1).

Mechanistically, the CIR can be rationalized as a rapid palladium/copper-catalyzed alkynylation reaction, followed by the slow base-catalyzed isomerization of a propargyl alcohol into an enone. In the past years, this new chalcone synthesis has been applied as an entry to novel three- and four-component syntheses of pyrazolines,[6] pyrimidines,[8] dihydrobenzo[*b*][1,4]-thiazepines and -diazepines,[9] pyrrols and furans,[10] and pyridines, pyrindines, and tetrahydroquinolines[11] in the sense of consecutive one-pot processes. These syntheses are based on subsequent Michael addition−cyclocondensations following the CIR. Because *N*-tosyl enimines can be well-considered as electron-deficient heterodienes that are perfectly suited for Diels−Alder reactions with inverse electron demand,[12] we could recently show that a CIR−cycloaddition sequence with a very electron-rich dienophile such as diethyl ketene acetal readily furnishes 2-ethoxy pyridines.[7] Here we report the extension of the one-pot synthesis of annelated pyridines based on a CIR−cycloaddition sequence with more nucleophilic *N*,*S*-ketene acetals as well as the absorption and emission properties of the resulting fluorescent pyrrolo[2,3-*b*]pyridines, [1,8]naphthyridines, and pyrido[2,3-*b*]azepines.

Results and Discussion

Annelated 2-amino pyridines, where the amino group is an *endo* constituent of the annelated saturated ring, are pharmaceutically intriguing structures. In particular, pyrrolo[2,3-*b*]-pyridines or 7-azaindolines,[13] [1,8]naphthyridines,[14] and pyrido-[2,3-*b*]azepines[15] have received considerable interest as a consequence of their broad pharmacological activity. Just recently, Zard has reported a fairly general synthetic access based on tin-free radical cyclizations.[16] On the basis of our experience in diversity-oriented heterocycle syntheses in a

SCHEME 2. Retrosynthetic Concept of a Consecutive One-Pot Three-Component Annelated 2-Amino Pyridine Synthesis[a]

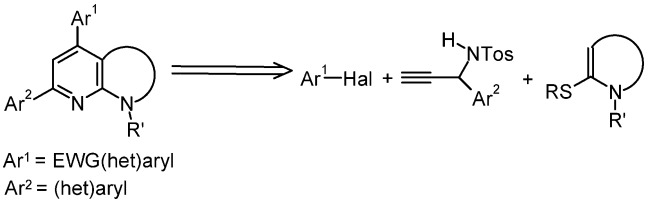

[a] Ar^1 = EWG(het)aryl; Ar^2 = (het)aryl.

SCHEME 3. One-Pot Three-Component Synthesis of Annelated 2-Amino Pyridines

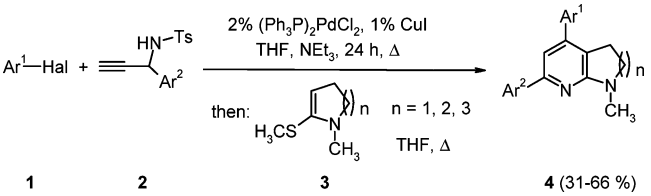

consecutive one-pot fashion (vide supra) and preliminary studies on CIR−cycloaddition sequences,[7,17] our retrosynthetic analysis of five-, six-, and seven-membered annelated amino pyridines based on the CI approach (Scheme 2) suggests enimines as key intermediates. Because *N*,*S*-ketene acetals are fairly electron-rich dienophiles[18] for [4+2] cycloadditions with inverse electron demand, a facile three-component CI−cycloaddition−aromatization synthesis of annelated 2-amino pyridines can be easily envisioned.

Thus, we submitted *p*-bromo benzonitrile (**1a**), 2-bromo pyridine (**1b**), or 2-bromo pyrimidine (**1c**) and *N*-[1-aryl-prop-2-ynyl] tosyl amides **2**,[7] and after some reaction time cyclic *N*,*S*-ketene acetals **3**,[19] to the reaction conditions of the CIR in a boiling mixture of THF and triethylamine. After aqueous workup, the annelated 2-aminopyridines **4** were obtained in 31−66% yield as light yellow crystalline solids (**4a**−**e**, **4g**−**i**) or brown oils (**4f**, **4j**; Scheme 3, Table 1).

The structures of the annulation products **4** were unambiguously assigned by ^{1}H, ^{13}C, COSY, and NOESY NMR experi-

(7) Dediu, O. G.; Yehia, N. A. M.; Müller, T. J. J. *Z. Naturforsch. B: Chem. Sci.* **2004**, *59*, 443−450.

(8) Müller, T. J. J.; Braun, R.; Ansorge, M. *Org. Lett.* **2000**, *2*, 1967−1970.

(9) (a) Braun, R. U.; Müller, T. J. J. *Tetrahedron* **2004**, *60*, 9463−9469. (b) Braun, R. U.; Zeitler, K.; Müller, T. J. J. *Org. Lett.* **2000**, *2*, 4181−4184.

(10) (a) Braun, R. U.; Müller, T. J. J. *Synthesis* **2004**, 2391−2406. (b) Braun, R. U.; Zeitler, K.; Müller, T. J. J. *Org. Lett.* **2001**, *3*, 3297−3300.

(11) (a) Dediu, O. G.; Yehia, N. A. M.; Oeser, T.; Polborn, K.; Müller, T. J. J. *Eur. J. Org. Chem.* **2005**, 1834−1848. (b) Yehia, N. A. M.; Polborn, K.; Müller, T. J. J. *Tetrahedron Lett.* **2002**, *43*, 6907−6910.

(12) (a) Sauer, J.; Wiest, H. *Angew. Chem., Int. Ed. Engl.* **1962**, *1*, 268. (b) Sauer, J.; Sustmann, R. *Angew. Chem., Int. Ed. Engl.* **1980**, *19*, 779−807. (c) Boger, D. L.; Patel, M. In *Progress in Heterocyclic Chemistry*; Suschitzky, H., Scriven, E. F. V., Eds.; Pergamon Press: Oxford, 1989, Vol. 1.

(13) (a) Desarbre, E.; Mérour, J.-Y. *Tetrahedron Lett.* **1996**, *37*, 43−46. (b) Taylor, E. C.; Pont, J. L. *Tetrahedron Lett.* **1987**, *28*, 379−382. (c) Beattie, D. E.; Crossley, R.; Curran, A. C. W.; Hill, D. G.; Lawrence, A. E. *J. Med. Chem.* **1977**, *20*, 718−721. (d) Robison, M. M.; Robison, B. L.; Butler, F. P. *J. Am. Chem. Soc.* **1959**, *81*, 743−747.

(14) For a recent pharmaceutical use of this class of compounds, see for example: (a) Hutchinson, J. H.; Halczenko, W.; Brashear, K. M.; Breslin, M. J.; Coleman, P. J.; Duong, L. T.; Fernandez-Metzler, C.; Gentile, M. A.; Fisher, J. E.; Hartman, G. D.; Huff, J. R.; Kimmel, D. B.; Leu, C. T.; Meissner, R. S.; Merkle, K.; Nagy, R.; Pennypacker, B.; Perkins, J. J.; Prueksaritanont, T.; Rodan, G. A.; Varga, S. L.; Wesolowski, G. A.; Zartman, A. E.; Rodan, S. B.; Duggan, M. E. *J. Med. Chem.* **2003**, *46*, 4790−4798. (b) Thomas Leonard, J.; Anbalagan, N.; Sadish Kumar, S.; Kishore Gnanasam, S.; Sridhar, S. *Biol. Pharm. Bull.* **2002**, *25*, 215−217. (c) Badawneh, M.; Ferrarini, P. L.; Calderoni, V.; Manera, C.; Martinetti, E.; Mori, C.; Saccomanni, G.; Testai, L. *Eur. J. Med. Chem.* **2001**, *36*, 925−934.

(15) Kavali, J. R.; Badani, B. V. *Farmaco* **2000**, *55*, 406−409.

(16) Bacqué, E.; El Qacemi, M.; Zard, S. Z. *Org. Lett.* **2004**, *6*, 3671−3674.

(17) D′Souza, D. M.; Rominger, F.; Müller, T. J. J. *Angew. Chem., Int. Ed.* **2005**, *44*, 153−158.

(18) Müller, K.; Sauer, J. *Tetrahedron Lett.* **1984**, *24*, 2541−2544.

(19) The *N*,*S*-ketene acetals were synthesized in a three-step sequence starting from the corresponding cyclic amides, according to: Yde, B.; Yousif, N. M.; Pedersen, U.; Thomsen, I.; Lawesson, S.-O. *Tetrahedron* **1984**, *40*, 2047−2052. By thionation with Lawesson's reagent, the amides were converted into the thiocarbonyl compounds in excellent yields (85−95%). After methylation with methyl iodide and recrystallisation from acetone, *S*-alkylated iodide salts (75−90%) were treated with potassium *tert*-butoxide to furnish the *N*,*S*-ketene acetals in moderate overall yields (35−65%).

TABLE 1. One-Pot Synthesis of Annelated 2-amino Pyridines 4

Entry	Aryl halide **1**	Propargyl *N*-tosyl amine **2**	*N*,*S*-ketene acetal **3**	2-Amino pyridines **4** (Yield)
1	Ar^1 = *p*-C_6H_4CN (**1a**)	Ar^2 = *p*-C_6H_4OMe (**2a**)	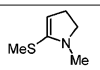 (**3a**)	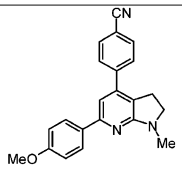 **4a** (64 %)
2	Ar^1 = 2-pyridyl (**1b**)	**2a**	**3a**	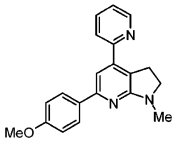 **4b** (49 %)
3	Ar^1 = 2-pyrimidyl (**1c**)	**2a**	**3a**	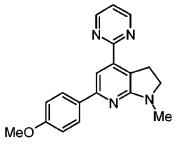 **4c** (66 %)
4	**1a**	**2a**	 (**3b**)	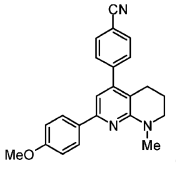 **4d** (31 %)
5	**1a**	Ar^2 = *p*-C_6H_4OPh (**2b**)	**3b**	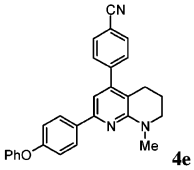 **4e** (43 %)
6	**1b**	**2a**	**3b**	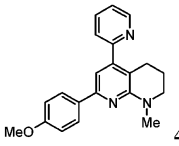 **4f** (48 %)
7	**1a**	**2a**	 (**3c**)	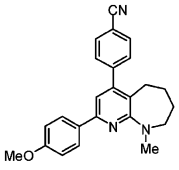 **4g** (52 %)
8	**1a**	**2b**	**3c**	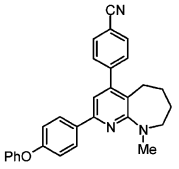 **4h** (43 %)
9	**1b**	**2a**	**3c**	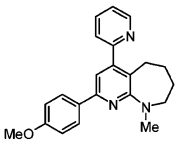 **4i** (52 %)
10	**1c**	**2a**	**3c**	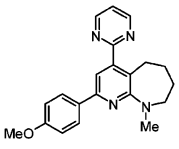 **4j** (56 %)

SCHEME 4. Mechanistic Rationale of the CI−Diels−Alder−Aromatization Sequence

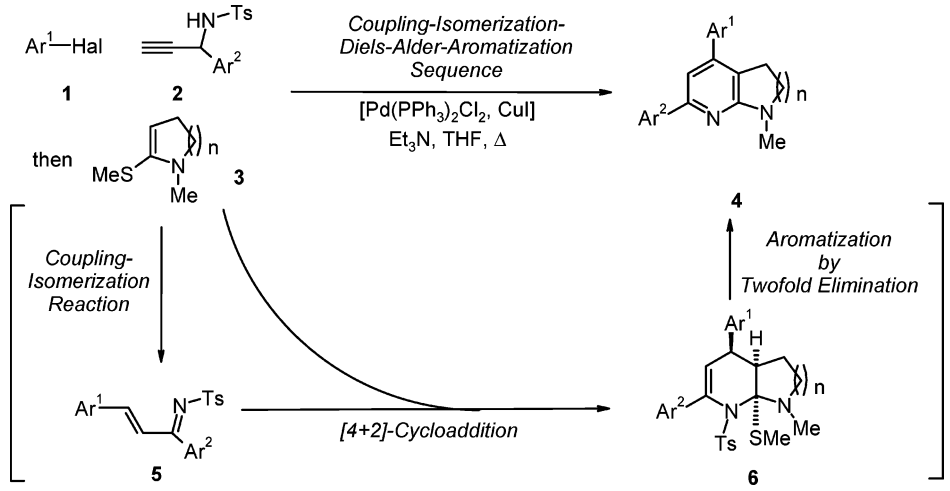

ments. Most characteristically, in the ^{1}H NMR spectra of **4**, the appearance of the methine singlets at δ 6.87−7.81 can be clearly attributed to the formation of pentasubstituted pyridyl core unit. In addition, the *N*-methyl protons are found as singlets at δ 3.02−3.22. Furthermore, the mass spectrometric and IR spectroscopic data are in full agreement with structural assignments. Finally, the structure of **4** was unambiguously supported by X-ray crystal structure analyses of compounds **4a**, **4c**, **4e**, **4h**, and **4i** (for ORTEP plots and structural data, see Supporting Information).[20]

Depending on the conformational bias of the annelated ring, the steric interactions force the acceptor-substituted (hetero)-aryl ring to twist out of coplanarity with the pyridyl core. The interplanar angle of the *p*-cyano phenyl ring and the central pyridine moiety increases from the pyrrolo[2,3-*b*]pyridine **4a** (43.5°) over the pyrido[2,3-*b*]azepine **4h** (60.7°, average between the independent molecules) to the [1,8]naphthyridine **4e** (88.6°). However, 2-pyridyl (**4i**, 39.4°) and 2-pyrimidyl substituents (**4c**, 6.8°) impose the least steric bias.

The tentative mechanism of this one-pot sequence can be described as follows (Scheme 4). After the CIR of the electron-deficient (hetero)aryl halide **1** and the propargyl tosyl amides **2** furnish an enimine **5**, the added *N*,*S*-ketene acetal **3** readily undergoes a [4+2] cycloaddition with inverse electron demand with **5** to give the annelated tetrahydropyridine **6** as the expected cycloadduct. However, under the reaction conditions, the 2-fold base-assisted elimination of tolylsulfinate and methyl mercaptane from **6** furnishes upon aromatization the annelated pyridine **4**.

All annelated 2-amino pyridines **4** absorb in the UV between 338 and 392 nm (Table 2). As a consequence of steric interactions between the annelated ring and the acceptor substituents in the 4-position of the central pyridine ring, the latter are twisted out of coplanarity with increasing conformational bias of the annulated moiety. Hence, the longest wavelength maxima are found for the pyrrolo[2,3-*b*]pyridines **4a**−**c**. Furthermore, these longest wavelength $\pi-\pi^*$ transitions, also reflecting the S_0-S_1 excitation, display dominant charge-transfer character with a significant mutual HOMO−LUMO overlap in a conformationally flexible 4-acceptor pyridyl framework. This is also nicely supported by calculations on the DFT level of theory (B3LYP G-31** density functional)[21] performed on the 2-pyrimidyl-substituted pyrrolo[2,3-*b*]pyridine **4c** (Figure 1) and the pyrido[2,3-*b*]azepine **4j** (Figure 2). The increase of steric bias upon enlarging the annelated five-membered ring to a seven-membered ring affects the orbital overlap and correlates with the absorption energy. Therefore, in all series the absorption maxima are bathochromically shifted upon increasing the acceptor strength of the substituent at the 4-position of the pyridine moiety from 2-pyridyl over *p*-cyanophenyl to 2-pyrimidyl.

TABLE 2. Selected UV/Vis and Fluorescence Properties (Recorded in Dichloromethane) of Annelated 2-Amino Pyridines 4

compound	absorption $\lambda_{max,abs}$ [nm] (ϵ)	emission $\lambda_{max,em}$ [nm]	quantum yield Φ_f [%]	$\Delta\nu^a$ [cm^{-1}]	fluorescence color
4a	**372** (3200) 310 (4400) 258 (21 900)	**469**	32	5600	green
4b	**360** (15 900) 276 (41 700) 248 (47 900)	**466** 512 sh	53	6300	green
4c	**392** (6500) 284 (12 900) 252 (40 700)	**468** 516 sh	63	4200	green
4d	**362** (5900) 306 (5900) 258 (31 600)	**438** 512 sh	12	4800	blue
4e	**364** (6600) 312 (5200) 258 (38 000)	**444** 518 sh	17	5000	blue
4f	**358** (6200) 256 (20 400)	**445** 513 sh	25	5500	blue
4g	**338** (3500) 260 (18 200)	**501**	24	9600	blue
4h	**340** (6600) 258 (38 900)	**495**	34	9200	blue
4i	**338**	**478**	26	8700	blue
4j	**348** (5500) 280 (14 800) 254 (23 400)	**511**	15	9200	green

^{a} $\Delta\tilde{\nu} = 1/\lambda_{max,\,abs} - 1/\lambda_{max,\,em}$ [cm^{-1}].

(20) Crystallographic data (excluding structure factors) for the structures reported in this paper have been deposited with the Cambridge Crystallographic Data Centre as supplementary publication nos. CCDC-297966 (**4a**), CCDC-297967 (**4c**), CCDC-297968 (**4e**), CCDC-297970 (**4h**), CCDC-297969 (**4i**). Copies of the data can be obtained free of charge on application to CCDC, 12 Union Road, Cambridge CB2 1EZ, U.K. (fax: + 44−1223/336−033; e-mail: deposit@ccdc.cam.ac.uk).

(21) As implemented in *PC Spartan Pro*, Wavefunction, Inc.: Irvine, CA, **2002**.

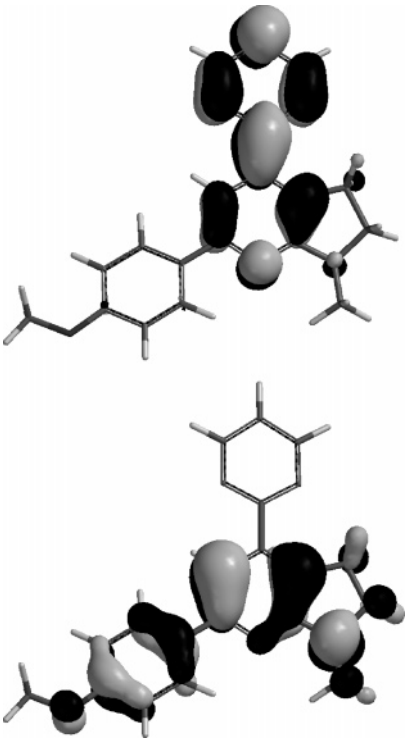

FIGURE 1. LUMO (top) and HOMO (bottom) of the pyrrolo[2,3-*b*]-pyrimidine **4c**.

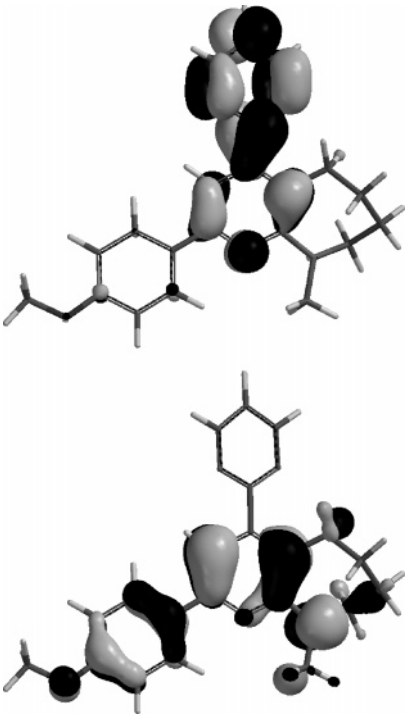

FIGURE 2. LUMO (top) and HOMO (bottom) of the pyrido[2,3-*b*]-azepine **4j**.

Furthermore, all annelated 2-amino pyridines **4** emit blue (**4d**−**i**) or green light (**4a**−**c**, **4j**) upon excitation at the corresponding absorption wavelengths (Table 2). The Stokes shifts are rather pronounced and lie between 4200 and 9600 cm^{-1}. For all representatives the quantum yields Φ_f were determined.[22] Pyrrolo[2,3-*b*]pyridines (**4a**−**c**) fluoresce with significantly higher quantum yields ($\Phi_f = 32-63\%$) than those of [1,8]naphthyridines (**4d**−**f**, $\Phi_f = 12-25\%$) and pyrido[2,3-*b*]azepines (**4g**−**j**, $\Phi_f = 15-34\%$). The longest wavelength emission maxima, however, are found in the series of pyrido-[2,3-*b*]azepines. As pointed out before for the absorption properties, the emission behavior is as well-affected by steric biases that control the efficiency of the spontaneous emission. Therefore, the charge-transfer character of the HOMO−LUMO transition responsible for the electronic absorption spectra is well-reflected in the torsion-dependent emission efficiency from the excited S_1 state.[23]

TABLE 3. Selected UV/Vis and Fluorescence Properties (Recorded in 0.1 M Acetate-Buffered DMSO Solution, $T = 298$ K) and Calculated HOMO and LUMO Energies of Pyrrolo[2,3-*b*]pyridines 4c and Pyrido[2,3-*b*]azepine 4j

compound	absorption $\lambda_{max,abs}$ [nm] (ϵ)	emission $\lambda_{max,em}$ [nm]	$\Delta\nu^a$ [cm^{-1}]	HOMO [eV]	LUMO [eV]	$\Delta_{HOMO-LUMO}$ [eV]
4c	**384** (2700)[b] 250 (8600)	**478**[b]	5100	−4.889	−1.544	3.345
4c−H^+	**392** (10 900)[c] 280 (15 100)	**482**[c]	4800	−8.563	−5.269	3.294
4j	**372** (9500)[b] 298 (11 800) 268 (12 300)	**478**[b]	6000	−4.911	−1.409	3.502
4j−H^+	**380** (6300)[d] 282 (7600)	**512**[d]	6800	−8.605	−5.224	3.381

[a] $\Delta\tilde{\nu} = 1/\lambda_{max,\,abs} - 1/\lambda_{max,\,em}$ [cm^{-1}]. [b] At pH 9. [c] At pH 1. [d] At pH 4.

The presence of a basic pyridyl nitrogen in the annelated 2-amino pyridines **4** invites a scrutinization of the pH dependence of the absorption and emission properties (Table 3). A discrete halochromicity can be detected for the 2-pyrimidyl-substituted pyrrolo[2,3-*b*]pyridine **4c** and the pyrido[2,3-*b*]-azepine **4j**, where bathochromic shifts of the longest wavelength absorption maxima are found by lowering the pH from pH 9 (**4c**, 384 nm; **4j**, 372 nm) to pH 1 (**4c**, 392 nm) or pH 4 (**4j**, 380 nm). This decrease of the HOMO−LUMO gap upon protonation is also reproduced in DFT calculations (B3LYP G-31** density functional)[21] on **4c**, **4c**−H^+, **4j**, and **4j**−H^+. For the couple **4c**/**4c**−H^+, the HOMO−LUMO gap reduces slightly upon protonation (**4c**, $\Delta_{HOMO-LUMO}$ 3.35 eV; **4c**−H^+, $\Delta_{HOMO-LUMO}$ 3.29 eV), whereas the decrease of the HOMO−LUMO gap is larger for the couple **4j**/**4j**−H^+ (**4j**, $\Delta_{HOMO-LUMO}$ 3.50 eV; **4j**−H^+, $\Delta_{HOMO-LUMO}$ 3.38 eV). However, the emission behavior is even more affected from protonation than from the absorption properties. The emission spectra of the 2-pyrimidyl-substituted pyrrolo[2,3-*b*]pyridine **4c** (Figure 3) and the pyrido-[2,3-*b*]azepine **4j** (Figure 4) display a quite different behavior upon altering the pH. Whereas for the pyrrolo[2,3-*b*]pyridine **4c**, the emission maximum only shifts slightly upon protonation (478 nm at pH 9; 482 nm at pH 1); for the pyrido[2,3-*b*]azepine **4j**, a significant bathochromic shift from 478 nm at pH 9 to 512 nm at pH 4 is observed. In the latter case, protonation of the pyridyl nitrogen is obviously occurring at higher pK_a as a consequence of an increase in basicity. Again, the steric bias causes a twist out of coplanarity of the 2-pyridyl substituent (vide supra) and, hence, exerts a diminished electron-withdrawing effect. The appearance of the fluorescence spectra of **4c** and **4j**, with shoulders at longer wavelengths, indicates that dual

(22) Determined with 7-diethylamino-4-methyl-chromen-2-one, coumarine 1, as a standard ($\Phi_f = 0.73$), see: Jones, G., II.; Jackson, W. R.; Choi, C. Y.; Bergmark, W. R. *J. Phys. Chem.* **1985**, *89*, 294−300.

(23) Valeur, B. *Molecular Fluorescence*; Wiley-VCH: Weinheim, Germany, **2002**.

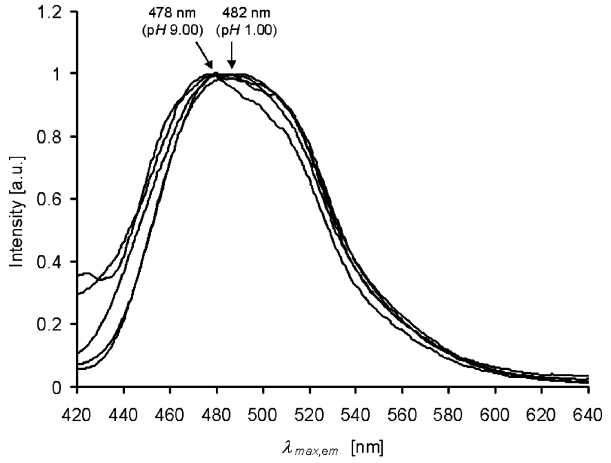

FIGURE 3. Emission maxima $\lambda_{max,em}$ [nm] (arbitrary units) of **4c** at pH 1.00, 2.00, 3.00, 4.00, and 9.00 (recorded in 0.1 M acetate-buffered DMSO solution, $T = 298$ K, $\lambda_{max,\,excitation} = 340$ nm).

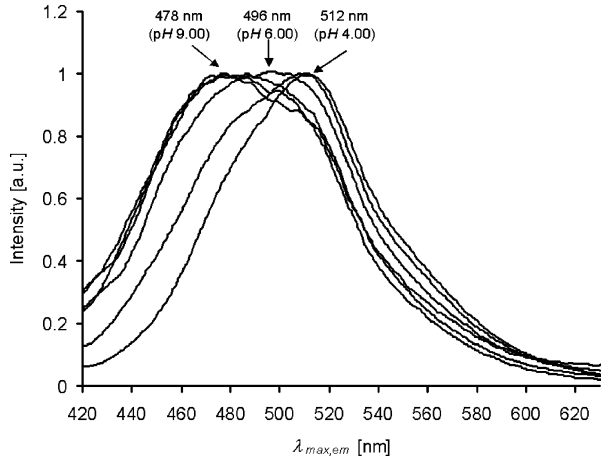

FIGURE 4. Emission maxima $\lambda_{max,em}$ [nm] (arbitrary units) of **4j** at pH 4.00, 5.00, 6.00, 7.00, 8.00, and 9.00 (recorded in 0.1 M acetate-buffered DMSO solution, $T = 298$ K, $\lambda_{max,\,excitation} = 340$ nm).

fluorescence of these donor−acceptor-substituted pyridines is obviously responsible for the variable pH sensitivity. In the former system, the 2-pyrimidyl substituent is already coplanar with the pyridine in the ground state, and the geometrical changes upon protonation are only minimal, whereas in the latter fluorophore, the S_0-S_1 excitation from the pyridyl core to the pyrimidine occurs with dominant charge-transfer character to an excited state that is coplanar and has to relax to a twisted state again. All this makes the pyrido[2,3-*b*]azepine **4j** a pH-sensitive fluorescence sensor that can be operative in neutral and weakly acidic media.

Conclusion

The mild reaction conditions of the CI sequence of electron-poor (hetero)aryl halides with 1-aryl propargyl *N*-tosylamines giving rise to enimines can be extended to a one-pot three-component synthesis of annelated 2-amino pyridines, such as pyrrolo[2,3-*b*]pyridines, [1,8]naphthyridines, and pyrido[2,3-*b*]-azepines, applying a cycloaddition with *N*,*S*-ketene acetals and subsequent aromatization. This methodology combines modern catalytic cross-coupling processes with pericyclic reactions and, therefore, opens new one-pot synthetic strategies as a consequence of mild reaction conditions and functional-group compatibility. All annelated 2-amino pyridines display pronounced blue or green fluorescence that can be controlled by reversible protonation in weakly acidic media for pyrido[2,3-*b*]azepines. Therefore, the fluorescence dyes, synthesized in a modular diversity-oriented fashion, can be ideal candidates for fluorescence labels for studying pH-dependent and pH-alternating cellular processes. Further studies are directed to the methodological development of novel multicomponent reactions, and the implementation of the fluorophores in biolabeling is currently under progress.

Experimental Section

General Procedure for the Coupling-Isomerization−Cycloaddition−Condensation Sequence to Annelated 2-Amino Pyridines, 4. A magnetically stirred solution of 1.00 mmol of halogen compound **1**, 1.05 mmol of propargyl tosyl amide **2**, 20 mg (0.02 mmol) of $(PPh_3)_2PdCl_2$, and 2 mg (0.01 mmol) of CuI in 3.5 mL of degassed triethylamine and 5 mL THF under nitrogen was heated to reflux temperature for 24 h (for a table with experimental details, see Supporting Information). After cooling to room temperature, a solution of 5 mmol of *N*,*S*-ketene acetals **3** in 1 mL of THF were added, and the reaction mixture was heated to reflux temperature for 12 h. After cooling to room temperature, 40 mL of ethyl acetate and 40 mL of water were added and stirring was continued for 5 to 10 min. The aqueous layer was extracted with ethyl acetate (4 × 15 mL), and the combined organic phases were dried with magnesium sulfate. After filtration, the solvents were removed in vacuo, and the residue was chromatographed on silica gel and recrystallized from a suitable solvent to give the analytically pure annelated 2-amino pyridine derivatives **4**.

6-(4-Methoxy-phenyl)-1-methyl-4-pyrimidin-2-yl-2,3−1*H*-pyrrolo[2,3-*b*]pyrimidine (4c). According to the GP, after chromatography on silica gel (hexane/acetone, 2.5:1) and recrystallization from diethyl ether, 210 mg (66%) of **4c** was isolated as yellow crystals: mp 190 °C. ^{1}H NMR (acetone-d_6, 300 MHz): δ 3.02 (s, 3H), 3.44−3.57 (m, 4H), 3.85 (s, 3H), 6.99 (d, $J = 9.0$ Hz, 2H), 7.20 (t, 1H), 7.43 (t, $J = 4.8$ Hz, 1H), 7.91 (s, 1H), 8.07 (d, $J = 8.9$ Hz, 2H), 8.93 (d, $J = 5.0$ Hz, 1H). ^{13}C NMR (acetone-d_6, $CDCl_3$, 75 MHz): δ 28.7 (CH_2), 32.9 (CH_3), 53.8 (CH_2), 55.6 (CH_3), 107.1 (CH), 114.6 (CH), 120.8 (CH), 122.7 ($C_{quat.}$), 128.4 (CH), 141.0 ($C_{quat.}$), 154.7 ($C_{quat.}$), 158.1 (CH), 160.9 ($C_{quat.}$), 161.0 ($C_{quat.}$), 165.8 ($C_{quat.}$). EI MS (70 eV, *m*/*z* (%)): 318.2 (M^+, 100), 303.2 ($M^+ - CH_3$, 7). IR (KBr): $\tilde{\nu}$ 3003, 2929, 2874, 2836, 1610, 1601, 1584, 1570, 1554, 1512, 1477, 1441, 1417, 1370, 1335, 1299, 1282, 1260, 1240, 1170, 1036, 807, 568 cm^{-1}. UV/vis (CH_2Cl_2) λ_{max} (ϵ): 252 (40 700), 284 (12 900), 392 (6500). Anal. Calcd for $C_{19}H_{18}N_4O$ (318.4): C, 71.68; H, 5.70; N, 17.60. Found: C, 71.58; H, 5.70; N, 17.86.

4-[2-(4-Methoxy-phenyl)-8-methyl-5,6,7,8-tetrahydro-[1,8]-naphthyridin-4-yl]pyridine (4f). According to the GP, after chromatography on silica gel (hexane/acetone, 3:1), 160 mg (48%) of **4f** were isolated as a brown oil. ^{1}H NMR (acetone-d_6, 300 MHz): δ 1.88 (m, 2H), 2.74 (t, $J = 6.3$ Hz, 2H), 3.24 (s, 3H), 3.45 (t, $J = 5.7$ Hz, 2H), 3.82 (s, 3H), 6.95 (d, $J = 8.9$ Hz, 2H), 7.05 (s, 1H), 7.35−7.37 (m, 1H), 7.51 (d, $J = 7.8$ Hz, 1H), 7.84 (t, $J = 7.9$ Hz, 1H), 8.05 (d, $J = 8.9$ Hz, 2H), 8.66−8.68 (m, 1H). ^{13}C NMR (acetone-d_6, 75 MHz): δ 22.3 (CH_2), 26.2 (CH_2), 37.1 (CH_3), 50.5 (CH_2), 55.5 (CH_3), 108.8 (CH), 113.9 ($C_{quat.}$), 113.0 ($C_{quat.}$), 114.5 (CH), 123.2 (CH), 124.7 (CH), 128.0 (CH), 128.3 (CH), 133.5 ($C_{quat.}$), 137.2 (CH), 148.0 ($C_{quat.}$), 150.0 (CH), 157.1 ($C_{quat.}$), 159.5 ($C_{quat.}$), 160.9 ($C_{quat.}$). IR (KBr): $\tilde{\nu}$ 2834, 1665, 1609, 1585, 1572, 1555, 1513, 1471, 1428, 1410, 1399, 1369, 1356, 1327, 1246, 1202, 1179, 1170, 1032, 831, 792 cm^{-1}. UV/vis (CH_2Cl_2) λ_{max} (ϵ): 256 (20 400), 358 (6200). HRMS (70 eV, EI): calcd for $C_{21}H_{21}N_3O$, 331.1685; found, 331.1679.

2-(4-Methoxy-phenyl)-9-methyl-4-pyrimidin-2-yl-6,7,8,9-tetrahydro-5*H*-pyrido[2,3-*b*]azepine (4j). According to the GP, after

chromatography on silica gel (hexane/acetone, 4:1) and recrystallization from diethyl ether, 194 mg (56%) of **4j** was isolated as a brown oil. ^{1}H NMR ($CDCl_3$, 300 MHz): δ 1.83−1.89 (m, 4H), 2.73−2.77 (m, 2H), 3.15 (s, 3H), 3.27−3.30 (m, 2H), 3.79 (s, 3H), 6.92 (d, J = 8.9 Hz, 2H), 7.17 (t, J = 4.9 Hz, 1H), 7.47 (s, 1H), 8.04 (d, J = 8.9 Hz, 2H), 8.78 (d, J = 4.9 Hz, 2H). ^{13}C NMR ($CDCl_3$, 75 MHz): δ 24.3 (CH_2), 27.3 (CH_2), 28.3 (CH_2), 40.4 (CH_3), 53.7 (CH_2), 55.1 (CH_3), 111.1 (CH), 113.6 (CH), 119.1 (CH), 121.9 ($C_{quat.}$), 127.6 (CH), 132.3 ($C_{quat.}$), 147.1 ($C_{quat.}$), 151.3 ($C_{quat.}$), 156.8 (CH), 159.7 ($C_{quat.}$), 162.0 ($C_{quat.}$), 167.1 ($C_{quat.}$). IR (KBr): $\tilde{\nu}$ 2932, 1608, 1589, 1566, 1547, 1513, 1492, 1443, 1418, 1368, 1350, 1333, 1296, 1247, 1191, 1179, 1032, 838, 813 cm^{-1}. UV/vis (CH_2Cl_2) λ_{max} (ϵ): 254 (23 400), 280 (14 800), 348 (5500). HRMS (70 eV, EI): calcd for $C_{21}H_{22}N_4O$, 346.1794; found, 346.1797.

Acknowledgment. The financial support of the Deutsche Forschungsgemeinschaft, the Morphochem AG, Munich, and the Fonds der Chemischen Industrie is gratefully acknowledged.

Supporting Information Available: Experimental details, computational data of **4c**, **4c**−$\mathbf{H}^+$, **4j**, and **4j**−$\mathbf{H}^+$, ^{1}H and ^{13}C NMR spectra of compounds **4**, and X-ray structure data and ORTEP plots of **4a**, **4c**, **4e**, **4g**, and **4i**. This material is available free of charge via the Internet at http://pubs.acs.org.

JO0602726